

Influence of polymorphism on charge transport properties in isomers of fluorenone-based liquid crystalline semiconductors.

Frédéric Lincker,^{a,b} André-Jean Attias,^b Fabrice Mathevet,^{*b} Benoit Heinrich,^c Bertrand Donnio,^{*c} Jean-Louis Fave,^d Patrice Rannou,^a and Renaud Demadrille^{*a}

^a INAC/SPrAM (UMR 5819 CEA-CNRS-Univ. J. Fourier-Grenoble 1), Laboratoire d'Electronique Moléculaire Organique et Hybride, 17 Rue des Martyrs, 38054 Grenoble Cedex 9, France. E-mail: renaud.demadrille@cea.fr

^b UPMC-UMR 7610, Laboratoire de Chimie des Polymères, Tour 44, 1^{er} étage, case courrier 185, 4, Place Jussieu, F-75252 Paris Cedex 05, France. Email: fabrice.mathevet@upmc.fr

^c IPCMS-UMR 7504, CNRS-Université de Strasbourg, 23, rue du Läss BP 43 F-67034 Strasbourg Cedex 2, France. Email: bdonnio@ipcms.u-strasbg.fr

^d UPMC-UMR 7588, Institut des Nanosciences de Paris, 4 Place Jussieu, F-75252 Paris Cedex 05, France.

S1. Material Synthesis

S1.1. General

All reagents and chemicals were purchased from Aldrich or Acros and used as received, except for THF which was distilled over sodium–benzophenone prior to use. Thin layer chromatography was performed on silica gel-coated aluminium plates with a particle size of 2–25 µm and a pore size of 60 Å. Merck 60 (70–230 mesh) silica was used for flash chromatography. All synthesised products were identified by ¹H and ¹³C NMR spectroscopy, as well as by elemental analysis. NMR spectra were recorded in chloroform-*d*, containing tetramethylsilane as internal standard, on a Bruker AC200 spectrometer. Elemental analyses (C, H, N, and S) were carried out by the Analytical Service of CNRS Vernaison (France) or by CRMPO at the University of Rennes 1 (France).

S1.2. Synthesis

B4OTF and **B5OTF** were prepared according by Suzuki-Miyaura cross-coupling reaction between 2,7-dibromofluoren-9-one and the appropriate alkylthiophene boronic esters and were purified by several runs of flash column chromatography followed by numerous recrystallisations in highly pure and metal-free acetonitrile. The general procedure can be briefly described as follows:

2,7-dibromofluorenone (1.92 mmol) and the appropriate boronate ester (4.34 mmol, 2.25 eq.) were placed in anhydrous DMF (20 mL). The mixture was stirred under argon for 10 min, then K₃PO₄ (4.24 mmol, 2.2 eq.) and Pd(PPh₃)₄ (0.173 mmol, 0.09 eq.) in 10mL of DMF were added. The mixture was kept at 100 °C for an additional period of 20 hours with constant stirring and then allowed to cool to room temperature. The product was then purified by column chromatography or by precipitation and filtration. In order to obtain high purity samples for TOF measurements, liquid crystalline semiconducting materials were purified by two runs of flash column chromatography and followed by three recrystallisations using highly pure and metal-free acetonitrile.

All the characterization data of **B4OTF** were identical to those reported in the following reference [R. Demadrille, P. Rannou, J. Bleuse, J-L. Oddou, A. Pron, M.Zagorska, *Macromolecules*, 2003, 36, 7045–7054].

2,7-bis(5-octylthien-2-yl)-fluoren-9-one (B5OTF): ¹H-NMR (CDCl₃, 200 MHz, ppm): δ 7.75 (d, 2H, *J*= 1.75 Hz), 7.56 (dd, 2H, *J*= 7.79 and 1.75 Hz), 7.52 (d, 2H, *J*= 7.79 Hz), 7.10 (d, 2H, *J*= 3.63 Hz), 6.67 (d, 2H, *J*= 3.63 Hz), 2.74 (t, 4H, *J*= 7.66 Hz), 1.57–1.68 (m, 4H), 1.10–1.40 (m, 20H), 0.75–0.95 (m, 6H). ¹³C-NMR (CDCl₃, 200 MHz, ppm): 193.45 (C=O), 146.56 (2C), 142.39 (2C), 140.36 (2C), 135.65 (2C), 135.08 (2C), 131.12 (2C), 125.22 (2C), 123.35 (2C), 121.07 (2C), 120.55 (2C), 31.84 (2C), 31.57 (2C), 30.27 (2C), 29.32 (2C), 29.20 (2C), 29.09 (2C), 22.63 (2C), 14.05 (2C). FT-IR (powder, ATR mode): 3080 (w), 2956 (m), 2919 (s), 2849 (s), 1722 (C=O, s), 1600 (m), 1583 (m), 1488 (s), 1465 (s), 1454 (s), 1430 (m), 1266 (m), 1172 (s), 834 (m), 800 (s), 782 (s), 721 (s). Elemental analysis: Calcd. for C₃₇H₄₄OS₂: C, 78.12 %; H, 7.80 %; S, 11.27 %. Found: C, 77.95 %; H, 7.74 %; S, 11.31 %.

S2. Thermotropic and structural Characterisations

S2.1 General

The optical textures of the mesophases were studied with a Leica polarizing microscope equipped with a Linkam LTS350 hot-stage and a linkam TMS94 temperature controller. The transition temperatures and enthalpies were measured by differential scanning calorimetry with a TA Instruments DSC-Q2000 instrument operated at a scanning rate of 10°C min⁻¹ during heating scan. The TGA measurements were carried out on a SDTQ 600 apparatus at scanning rate of 10°C min⁻¹. The XRD patterns were obtained with two different experimental set-ups. In all cases, a linear monochromatic Cu-K_{α1} beam ($\lambda = 1.5405 \text{ \AA}$) was obtained using a sealed-tube generator (900 W) equipped with a bent quartz monochromator. In all cases, the crude powder was filled in 1 mm diameter Lindemann capillaries.. The initial set of diffraction patterns was recorded on an image plate for which periodicities up to 80Å can be measured. Within this configuration, the sample temperature was controlled within ±0.3°C in the 20 to 350°C temperature range. The second set of diffraction patterns was recorded with a curved Inel CPS120 counter gas-filled detector linked to a data acquisition computer (periodicities up to 60Å) or was measured on image plates (periodicities up to 100Å). Within this configuration, the sample temperature was controlled within ±0.05°C in the 20 to 200°C temperature range. In each case, exposure times were varied from 1 to

24 h.

S2.2 Polarized-light Optical Microscopy (POM)

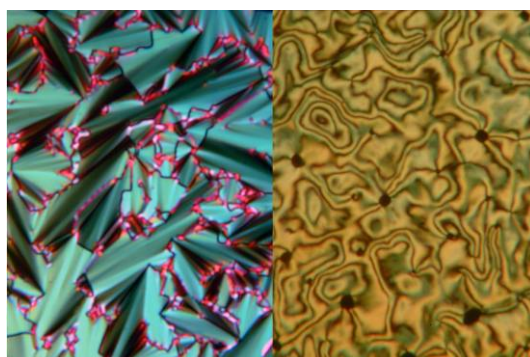


Fig. S2.2.1 Optical textures observed for **B4OTF** at 120°C with sulfochromic acid (*fan-shaped*, left) and silane (OTS) (*Schlieren*, right) glass slides treatment.

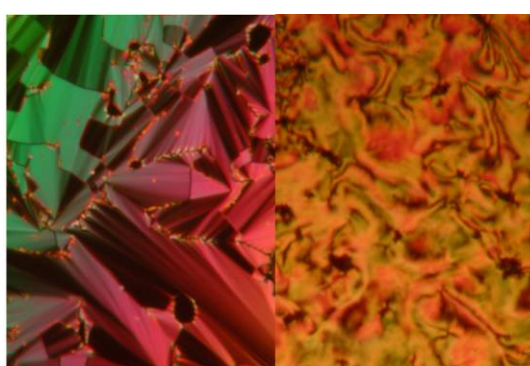
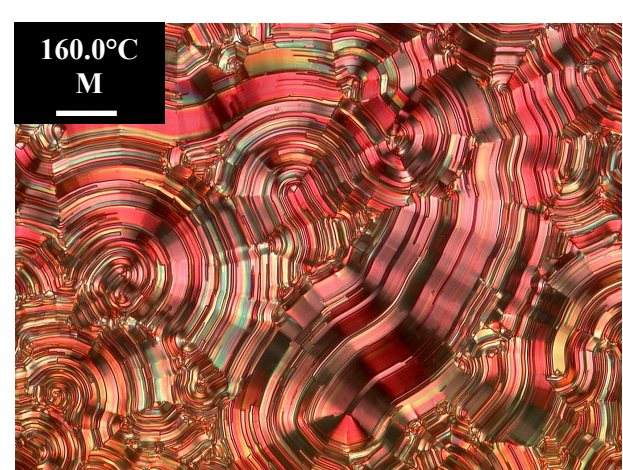
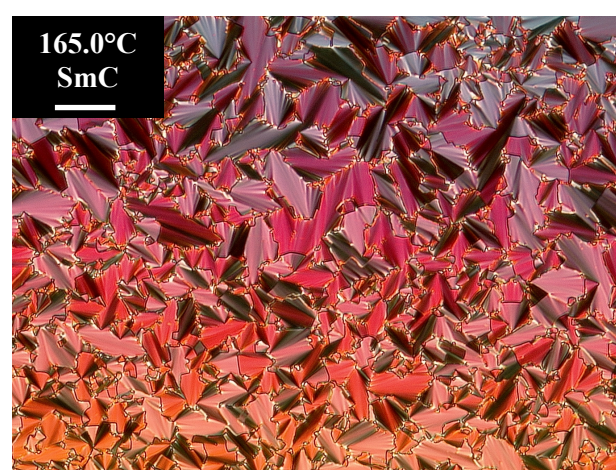


Fig. S2.2.2 Optical textures observed for **B5OTF** at 200°C with sulfochromic acid (*fan-shaped*, left) and silane (OTS) (*Schlieren*, right) glass slides treatment.



Fig. S2.2.3 Optical textures observed for **B5OTF** at 160°C with sulfochromic acid glass slides treatment (*spherulitic texture*).



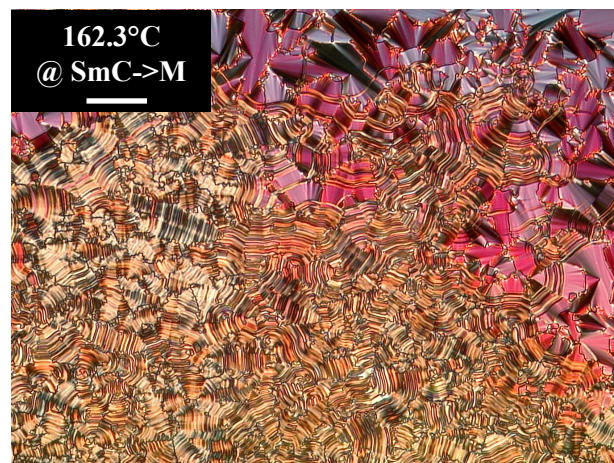


Fig. S2.2.4 Optical textures observed for **B5OTF** at 165°C (Top left POM microphotograph: *Broken focal-conic-fan texture of its SmC mesophase*), at 162.3°C (bottom middle POM microphotograph taken at the SmC->M phase transition: *transitory co-existence of textures of the SmC and M phases*), and at 160.0°C (top right POM microphotograph: *Spherulitic texture of its M mesophase*) with sulfochromic acid glass slides treatment. The scale bar is worth 50 microns.

S2.3 Differential Scanning Calorimetry study (DSC)

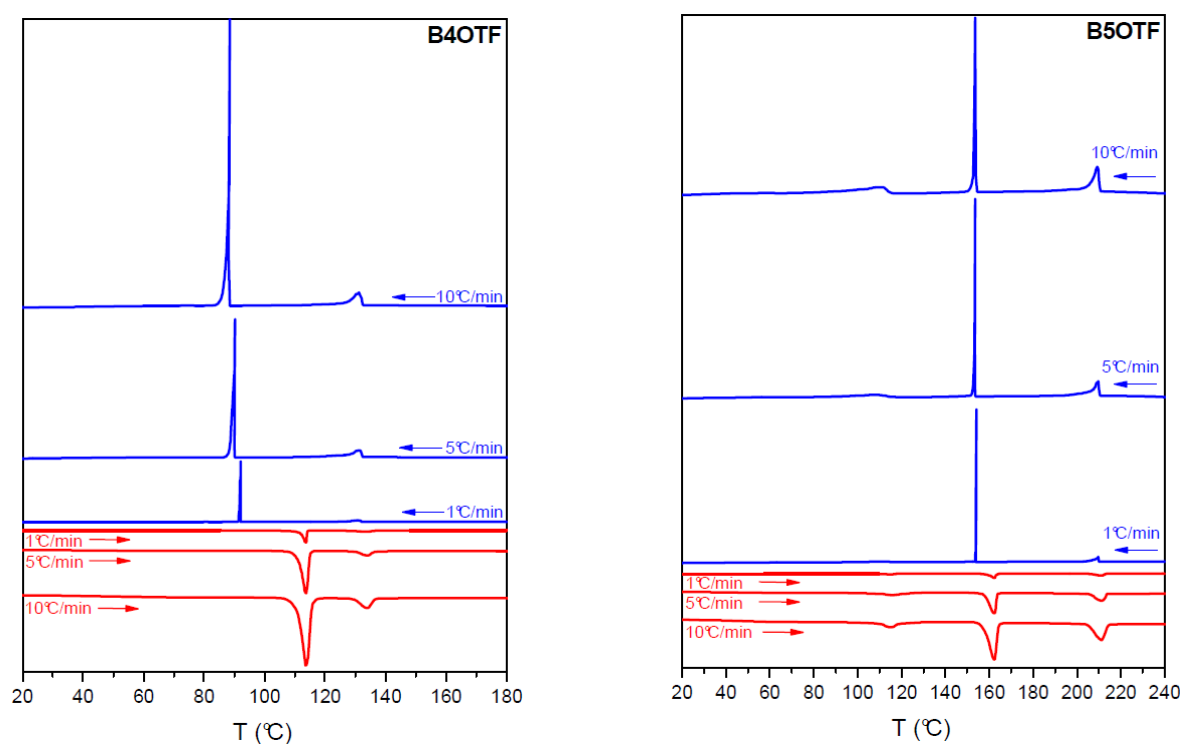


Fig. S2.3.1 DSC traces for **B4OTF** and for **B5OTF** recorded at scanning rates of 10, 5, and $1^{\circ}\text{C}\cdot\text{min}^{-1}$.

S2.4 X-ray diffraction experiments

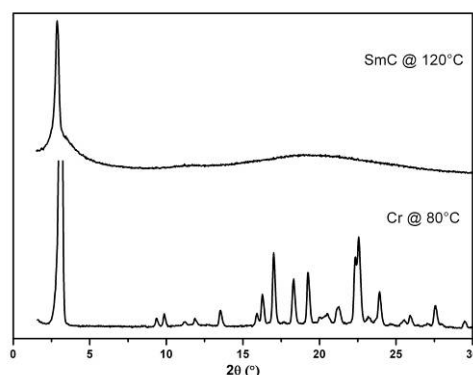


Fig. S2.4.1 Temperature dependence of X-ray diffraction patterns (powder) of **B4OTF** at 120°C and 80°C.

Compounds	hkl ^a	2θ _{obs} [°] ^a	d _{obs} [Å] ^a	T [°C] ^a	Ψ [°] ^a
B4OTF	001	2.88	30.65	120	46.25
B5OTF	001	2.93	30.13	190	47.17

^a hkl: Miller indices; θ_{obs}, and d_{obs} are the observed diffraction angles and spacings; T: Measurement temperature; Ψ: tilt angle inside the smectic C layer.

Table S2.4.1: Reflections in the small angles region for **B4OTF** and **B5OTF** in their respective SmC phases at 120°C and 190°C, respectively.

Compounds	hkl ^a	2θ _{obs} [°] ^a	d _{obs} [Å] ^a	T [°C] ^a	Ψ [°] ^a
B4OTF	001	3.08	28.66	40	49.73
B5OTF	001	2.88	30.65	40	46.25

^a hkl: Miller indices; θ_{obs}, and d_{obs} are the observed diffraction angles and spacings; T: Measurement temperature; Ψ: tilt angle inside the smectic C layer.

Table S2.4.2: Interlamellar spacing for **B4OTF** and **B5OTF** in their respective Cr phases at 40°C.

While high intensity peaks related to the lamellar periodicity (i.e. (001) reflections) are observed for both **B4OTF** and **B5OTF** in their respective SmC and SmC+M phases, no clear signatures of second order peaks have been observed. Our proposal for a lamellar organization is further supported by the appearance of higher order peaks within the M phase of **B5OTF**. We tentatively rationalize this experimental fact by considering an unfavorable electronic density profile within the lamellar organization which impedes, with our laboratory experimental set-up, its occurrence (002) due to the fact that the total length of the alkyl chains is roughly that of the pi-conjugated central core.

S3. Time Of Flight (TOF) sample fabrication and characterisation

S3.1. General

Transient hole photocurrents were measured with a conventional TOF setup using a nitrogen laser ($\lambda = 337$ nm, sub-ns pulse duration, excitation density: $30 \mu\text{J} \cdot \text{pulse}^{-1} \text{cm}^{-2}$, repetition rate: 1.5 Hz) as the excitation source. TOF samples were prepared by capillarity filling ca. 5-6 mg of BO4TF and B5OTF in their isotropic phases into liquid crystal cells consisting of two indium tin oxide-coated glass slides (ITO) separated by 9 μm spacers (Instec). ITO electrodes effective area was 1 cm^2 . Transient photocurrent vs. temperature and electric field were recorded and averaged on a digital oscilloscope. Transit times were determined from double logarithmic plots.

Charge carrier mobility as a function of temperature was determined during controlled cooling from isotropic state to crystal state. Mobility values were extracted from transient photocurrent curves recorded every 2, 5 or 10°C after a temperature stabilization period of ca. 2-3 min at each selected temperature. Once can therefore consider that the measurements were performed in quasi steady-state conditions. Moreover, the same electric field was applied for all temperatures investigated.

S3.2. Time Of Flight (TOF)

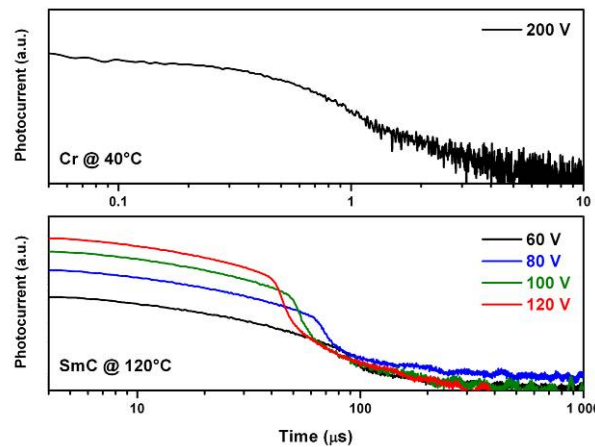


Fig. S3.2.1 Transient hole photocurrent curves of B4OTF in the crystalline Cr and SmC phases at different voltage.

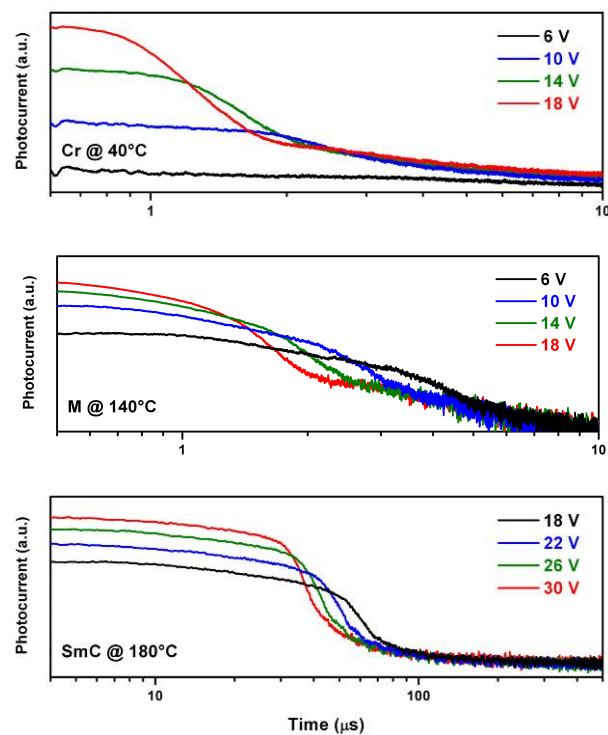


Fig. S3.2.2 Transient hole photocurrent curves of B5OTF in the Cr, M, and SmC phases at different voltage